

# Condensed Matter

Alexander Byrne

Almost Out

## 1 Periodic Structure

### 1.1 Bravais Lattice

The structure of a crystal is the convolution of a *Bravais lattice* and a *basis*. The basis consists of the simplest repeating unit of atoms – for example, an NaCl unit; the Bravais lattice is a repeating 3D array of  $\delta$  functions, at locations known as lattice points. There are 14 types of Bravais lattices, of which three concern us: Primitive cubic (P), Body-centred cubic (I or BCC) and Face-centred cubic (F or FCC).

Any repeating unit in a crystal is called a “unit cell”; it is endowed the description of “primitive” if it contains just one lattice point. Of the above, only the P lattice (suggestibly) is primitive; BCC and FCC contain 2 and 4 lattice points resp. The *Wigner-Seitz construction* generates a primitive unit cell in any crystal structure.

Unit cells are defined by three basis vectors  $\mathbf{a}$ ,  $\mathbf{b}$ , and  $\mathbf{c}$ , so that any point  $\mathbf{r}$  in the crystal may be described as  $\mathbf{r} = u\mathbf{a} + v\mathbf{b} + w\mathbf{c}$ , or in the form  $[uvw]$  as favoured by crystallographers. In this notation, negative values (e.g.  $\mathbf{a} - \mathbf{b} - 2\mathbf{c}$ ) are denoted with overbars:  $[1\bar{1}\bar{2}]$ . In many cases, lots of vectors and directions are related to each other by symmetry: for instance, in the P lattice, the vectors  $[100]$ ,  $[001]$ ,  $[0\bar{1}0]$  etc. are symmetrically equivalent, and the set is denoted  $\langle 100 \rangle$ .

A set of parallel planes in a crystal are described using *Miller indices*  $(hkl)$ . Consider the first such plane away from the origin: the indices are determined by where this plane intersects the three crystallographic axes. For instance, if the plane intersects the axes at  $\mathbf{a}$ ,  $\mathbf{b}/2$ ,  $\mathbf{c}/3$ , then the set of parallel planes have Miller indices  $(123)$ . As with vectors in general, there may be many symmetrically equivalent planes; the set is denoted  $\{hkl\}$ . To summarise:

- $[hkl]$  – a vector
- $\langle hkl \rangle$  – a set of symmetry-related vectors
- $(hkl)$  – a plane
- $\{hkl\}$  – a set of symmetry-related planes

## 1.2 Reciprocal Lattice

The Fourier transform of the Bravais lattice is the reciprocal lattice. Any function that can represent a property of the crystal must have a periodicity so that on translating from  $\mathbf{r} \rightarrow \mathbf{r} + [hkl]$  with  $h, k, l \in \mathbb{Z}$ , the function is unchanged. A basis for the reciprocal lattice vectors is:

$$\mathbf{A} = 2\pi \frac{\mathbf{b} \times \mathbf{c}}{\mathbf{a} \cdot \mathbf{b} \times \mathbf{c}} \quad \mathbf{B} = 2\pi \frac{\mathbf{c} \times \mathbf{a}}{\mathbf{a} \cdot \mathbf{b} \times \mathbf{c}} \quad \mathbf{C} = 2\pi \frac{\mathbf{a} \times \mathbf{b}}{\mathbf{a} \cdot \mathbf{b} \times \mathbf{c}}$$

In this way, any crystallographically periodic function can be expressed as:

$$f(\mathbf{r}) = \sum_{h,k,l} F_{hkl} e^{i\mathbf{G}_{hkl} \cdot \mathbf{r}}$$

where  $\mathbf{G}_{hkl} = h\mathbf{A} + k\mathbf{B} + l\mathbf{C}$ , are often referred to as “G-vectors”; these form the reciprocal lattice. This has the correct periodicity because  $\mathbf{A}_i \cdot \mathbf{a}_j = 2\pi\delta_{ij}$  so if  $\mathbf{r}$  is a linear combination of the lattice vectors  $\mathbf{a}_i$ , then the exponent will be a multiple of  $e^{2\pi i} = 1$ .  $\mathbf{G}_{hkl}$  is perpendicular to the  $(hkl)$  planes.

## 1.3 Diffraction Experiments

X-rays and thermal neutrons beams have the right wavelengths to diffract from a crystal lattice. When a wavefront of wavevector  $\mathbf{k}_i$  is incident on an atom, it generates secondary wavelets. For a strong resultant beam of wavevector  $\mathbf{k}_f$ , the phase difference between the secondary wavelets from two adjacent atoms (easily shown to be  $(\mathbf{k}_f - \mathbf{k}_i) \cdot \mathbf{r}$  where  $\mathbf{r}$  is the vector between the two atoms) should be a multiple of  $2\pi$ . As such,  $\mathbf{k}_f = \mathbf{k}_i + \mathbf{G}_{hkl}$  for some  $h, k, l$ .

However, conservation of energy adds the further requirement that  $|\mathbf{k}_f| = |\mathbf{k}_i|$ , so the addition of  $\mathbf{G}_{hkl}$  must not change the magnitude of the  $\mathbf{k}$  vector – there is an isosceles triangle formed between the  $\mathbf{k}_i$ ,  $\mathbf{k}_f$  and  $\mathbf{G}_{hkl}$ . This is

best visualised using the *Ewald sphere* construction. Often there is no such  $\mathbf{G}_{hkl}$ , and so there will be no diffraction.

Diffraction experiments are either *single-crystal*, or *powder*. Single-crystal diffraction is used to determine structures: the beams form spots, with angles and intensities relating to the crystal structure. Powder diffraction uses a sample of many small crystals in all possible orientations: the beams form rings, whose angles may identify phases or structure changes.

## 2 Phonons

### 2.1 Monatomic Crystals

It is hard to describe the vibrational motion of the atoms in a crystal atom-by-atom, so a normal modes approach is used; this should be done quantum-mechanically, but apparently a classical analysis gives the same answers. The energy of each normal mode is  $(n + 1/2)\hbar\omega$  where  $n$  is said to be the number of *phonons* in the mode.

By considering the forces in a 1D harmonic chain with interatomic separation  $a$ , and positing a longitudinal displacement form  $u_n = u_0 e^{i(nqa - \omega t)}$ , we arrive at the dispersion relation:

$$\omega = 2\omega_0 \left| \sin\left(\frac{qa}{2}\right) \right|$$

where  $\omega_0 = \sqrt{\alpha/m}$ . This dispersion relation is only meaningfully defined for  $q \in (-\pi/a, \pi/a)$  (the *First Brillouin Zone*), as any larger wavevectors would have a phase difference of more than  $\phi > 2\pi$  between neighbouring atoms, which is totally equivalent to a phase difference of  $\phi - 2\pi \in (-\pi, \pi)$ , as it doesn't matter what the wave looks like *between* the atoms as there's nothing there. Thus a phonon with wavevector  $\mathbf{q}$  is entirely equivalent to one with wavevector  $\mathbf{q} + n\mathbf{G}_{hkl}$ . As always, the velocity of a phonon is given by  $\frac{\partial\omega}{\partial q}$ .

The long-wavelength (low- $q$ ) limit gives:

$$\lim_{q \rightarrow 0} \omega = \omega_0 a q \Rightarrow v \rightarrow \omega_0 a$$

which it turns out is the same as when one considers the speed of sound in a homogeneous material – for long wavelengths the atomic structure of the material is inconsequential.

For wavelengths near the edge of the Brillouin zone, the gradient of the dispersion relation approaches 0 and a standing wave is achieved as the phase difference between neighbours reaches  $\pi$ .

Discrepancies between the theory above and experiment can be due to: anharmonicity of intermolecular forces; next-nearest-neighbour interactions.

One can assign a momentum  $\hbar\mathbf{q}$  to a phonon, which enables explanations of coalescence and splitting of phonons. It is possible for a coalescence to produce a phonon with a  $\mathbf{q}$  outside of the 1BZ, so one ought to subtract  $\mathbf{G}$  vectors until it returns to the 1BZ. In this sense, “crystal momentum” is defined only up to  $\hbar$  times a number of  $\mathbf{G}$  vectors.

If one probes a crystal with a thermal neutron, it can excite or annihilate a phonon. One can then use the changes in momentum ( $\hbar\mathbf{q}+n\mathbf{G}$ ) and energy ( $\hbar\omega$ ) of the neutron to analyse the phonon properties.

## 2.2 Diatomic Crystals

For a crystal with two atoms of mass  $m_A, m_B < m_A$ , the analysis leads to the dispersion relation:

$$\omega = \sqrt{\frac{\alpha}{m_A m_B} \left[ m_A + m_B \pm \sqrt{(m_A + m_B)^2 - 4m_A m_B \sin^2(qa)} \right]}$$

Most notably, there are now two branches – the higher frequency branch is termed the *optical branch* as it interacts strongly with EMR if the crystal is polar; the lower branch is termed the *acoustic branch*, as it corresponds to sound waves in the low- $q$  limit. In addition, the size of the Brillouin zone has halved, as the periodicity has become  $2a$ ; the appearance of two branches can be understood using the concept of “backfolding”.

In different regimes, we have:

$$\begin{aligned} \lim_{q \rightarrow 0} \omega_o &\rightarrow \sqrt{\frac{2\alpha}{\mu}} & \text{where } \mu &\equiv \frac{m_A m_B}{m_A + m_B} \\ \lim_{q \rightarrow 0} \omega_a &\rightarrow \sqrt{\frac{2\alpha}{m_A + m_B}} qa & \Rightarrow \lim_{q \rightarrow 0} v &\rightarrow \sqrt{\frac{2\alpha}{m_A + m_B}} a \\ \lim_{q \rightarrow \pi/2a} \omega_o &\rightarrow \sqrt{\frac{2\alpha}{m_B}} \\ \lim_{q \rightarrow \pi/2a} \omega_a &\rightarrow \sqrt{\frac{2\alpha}{m_A}} \end{aligned}$$

On solving for the different amplitudes of oscillation, we see that another difference between optical and acoustic modes is: for optical modes, neighbouring atoms move out of phase; for acoustic modes they are in phase. At the zone boundary, we end up with only one mass moving (the one present in the limiting form of  $\omega$ ), and the other stationary.

For 3D systems, the above all still applies, but transverse oscillations now also exist. These “T” modes are described in a similar way to the “L” modes we have considered, but with effectively a lower  $\alpha$  and thus lower frequencies; the dispersion relations are usually similar in form though.

## 3 Thermal Properties

### 3.1 Heat Capacity

The average energy stored in a single mode of frequency  $\omega$  at temperature  $T$  is given by Planck’s formula:

$$\langle E \rangle = \frac{\hbar\omega}{e^{\beta\hbar\omega} - 1}$$

where  $\beta = 1/k_B T$ . The total internal energy of the crystal is then given by:

$$U = \sum_i^N \frac{\hbar\omega_i}{e^{\beta\hbar\omega_i} - 1} \rightarrow \int \frac{\hbar\omega}{e^{\beta\hbar\omega} - 1} dN = \int \frac{\hbar\omega}{e^{\beta\hbar\omega} - 1} g(\omega) d\omega$$

where  $g(\omega)$  the “density of states”, is defined by  $g(\omega) d\omega$  being the number of states with frequencies on  $[\omega, \omega + d\omega)$ . This is estimated using *Debye Theory*, discussed below.

Suppose the overall crystal has dimensions  $X, Y, Z$ , and that the boundary conditions are “reflecting”. This gives that the possible values of  $\mathbf{q}$  are:

$$\mathbf{q} = \left( \frac{n_x\pi}{X}, \frac{n_y\pi}{Y}, \frac{n_z\pi}{Z} \right)$$

where  $(n_x, n_y, n_z)$  are all positive. Each possible value of  $\mathbf{q}$  thus takes up a volume  $\pi^3/V$  in  $\mathbf{q}$ -space, where  $V = XYZ$  is the volume of the crystal. Given that the number of states with each value of  $\mathbf{q}$  is 3 (one longitudinal, two transverse), the number of states with a wavevector magnitude between  $q$  and  $q + dq$  is:

$$dN = 3 \frac{4\pi q^2 dq / 8}{\pi^3/V} = \frac{3V}{2\pi^2} q^2 dq$$

and so the number of states with a frequency between  $\omega$  and  $\omega + d\omega$  is:

$$dN = \frac{3V}{2\pi^2} q^2 \frac{dq}{d\omega} d\omega = \frac{3V\omega^2}{2\pi^2 v_s^3} d\omega \Rightarrow g(\omega) = \frac{3V}{2\pi^2 v_s^3} \omega^2$$

where  $\omega = v_s q$  defines sort of the speed of sound [Debye assumes this to be independent of frequency, and related to the transverse and longitudinal speeds by:

$$\frac{3}{v_s} = \frac{2}{v_T} + \frac{1}{v_L}$$

.] We are now in a position to integrate the earlier expression to obtain  $U$ , but we should not integrate up to infinity, as there are only  $3N$  modes in the entire crystal. The *Debye frequency*  $\omega_D$  is the highest possible phonon frequency:

$$3N \equiv \int_0^{\omega_D} g(\omega) d\omega = \frac{V}{2\pi^2 v_s^3} \omega_D^3 \Rightarrow \omega_D = (6\pi^2 v_s^3 N/V)^{1/3} = (6\pi^2 v_s^3 n)^{1/3}$$

We then have:

$$U = \int_0^{\omega_D} \frac{\hbar\omega}{e^{\hbar\omega/kT} - 1} \frac{3V}{2\pi^2 v_s^3} \omega^2 d\omega = \frac{3V\hbar}{2\pi^2 v_s^3} \int_0^{\omega_D} \frac{\omega^3}{e^{\hbar\omega/kT} - 1} d\omega$$

which isn't very easy. The heat capacity  $C \equiv \frac{\partial U}{\partial T}$  is given by:

$$\begin{aligned} C &= \frac{3V\hbar}{2\pi^2 v_s^3} \int_0^{\omega_D} \frac{\omega^3}{(e^{\hbar\omega/kT} - 1)^2} \frac{\hbar\omega}{kT^2} e^{\hbar\omega/kT} d\omega \\ &= \frac{3V\hbar^2}{2\pi^2 v_s^3 kT^2} \int_0^{\omega_D} \frac{\omega^4}{(e^{\hbar\omega/kT} - 1)^2} e^{\hbar\omega/kT} d\omega \\ &= \frac{3V\hbar^2}{2\pi^2 v_s^3 kT^2} \frac{k^5 T^5}{\hbar^5} \int_0^{\theta_D/T} \frac{x^4 e^x}{(e^x - 1)^2} dx \\ &= \frac{V}{6N\pi^2 v_s^2} \left(\frac{kT}{\hbar}\right)^3 9Nk \int_0^{\theta_D/T} \frac{x^4 e^x}{(e^x - 1)^2} dx \\ &= 9Nk \left(\frac{T}{\theta_D}\right)^3 \int_0^{\theta_D/T} \frac{x^4 e^x}{(e^x - 1)^2} dx \end{aligned}$$

where  $\hbar\omega_D = k\theta_D$ ; the *Debye temperature*. This gives different results in different regimes. At high temperatures the upper bound is small and so the integrand is small over the whole integration range:

$$\lim_{T \rightarrow \infty} C = 9Nk \left(\frac{T}{\theta_D}\right)^3 \int_0^{\theta_D/T} \frac{x^4}{x^2} dx = 3Nk$$

which is independent of temperature and was in fact known experimentally before, as the *Dulong-Petit Law*. One could also see this as arising from the fact that for high-temperatures the energy of each mode tends to  $kT$ , and

there are  $3N$  modes so  $U = 3NkT, C = 3Nk$ . For low temperatures, the integral goes to infinity, apparently giving  $4\pi^4/15$ , so:

$$\lim_{T \rightarrow 0} C = 9NK \left( \frac{T}{\theta_D} \right)^3 \frac{4\pi^4}{15} = \frac{12\pi^4}{5} Nk \left( \frac{T}{\theta_D} \right)^3$$

which is proportional to  $T^3$ , as experiment corroborates.

Discrepancies may arise from: high- $\omega$  modes with non-linear dispersion relations; more complicated  $g(\omega)$  forms.

### 3.2 Thermal Conductivity

The thermal conductivity  $\kappa$  of an insulator is given by the formula:

$$\kappa = \frac{1}{3} C \langle c \rangle l$$

where  $C$  is the heat capacity,  $\langle c \rangle$  is the average phonon speed, and  $l$  is the phonon mean free path. The latter is limited by *phonon scattering*, which can be due to: geometric scattering, off of impurities or boundaries (independent of  $T$ ); phonon-phonon scattering, off of other phonons (only possible due to anharmonicity,  $\propto T^{-1}$  at high  $T$ ).

Phonon-phonon scattering can be *normal* or *umklapp*. Umklapp scattering occurs when the coalescence of two phonons brings the resultant phonon outside of the 1BZ. After subtracting  $\mathbf{G}$ -vectors to return to the 1BZ, the resultant  $\mathbf{q}$  is often in a completely different direction – umklapp scattering causes strong randomisation of the phonons and reduces  $l$ . However, this can only occur frequently if there are lots of phonons reasonably close to the edge of the 1BZ in the first place (otherwise most will simply scatter normally), and this is only the case at high temperatures. Therefore, as the temperature decreases, the umklapp processes becomes less prevalent and the conductivity actually rises above the  $T^{-1}$  asymptote.

As a result, a plot of  $\kappa$  against  $T$  often rises as  $T^3$  for low temperatures (due to  $C$ ) and then falls onto a  $T^{-1}$  asymptote for higher temperatures (due to  $l$ ).

## 4 The Free Electron Model

Unlike previously, where we have been thinking about the motions of the *atoms* in the crystal, we now move on to looking at what the *electrons* are doing in a metal. This is reasonably well described by the *free electron model*, which makes predictions about a wide range of properties of the metal, some of which more accurate than others. The model assumes:

- The nuclei create a uniform background potential
- There is no electron-electron repulsion
- The Pauli Exclusion Principle

As with the Debye theory, we begin by assuming a volume  $V = XYZ$ . Using cyclic boundary conditions this time, the possible electron states are then:

$$\Psi(x, y, z) \propto \sin\left(\frac{2\pi n_x x}{X}\right) \sin\left(\frac{2\pi n_y y}{Y}\right) \sin\left(\frac{2\pi n_z z}{Z}\right)$$

so we have:

$$\mathbf{k} = \left(\frac{2\pi n_x}{X}, \frac{2\pi n_y}{Y}, \frac{2\pi n_z}{Z}\right)$$

where  $n_x$  etc can apparently each be negative as well, so all 8 octants of  $k$ -space will be used. Each point in the  $k$ -space lattice has a volume  $8\pi^3/V$  as before, and the PEP says that each  $k$ -state can be occupied by 2 electrons. The number of electrons in states between  $k$  and  $k + dk$  is therefore:

$$dN = 2 \frac{4\pi k^2 dk}{8\pi^3/V} = \frac{Vk^2}{\pi^2} dk$$

The number of electrons in states between  $E$  and  $E + dE$  is then calculated as follows:

$$\begin{aligned} E &= \frac{\hbar^2 k^2}{2m} & \Rightarrow dE &= \frac{\hbar^2 k}{m} dk \\ \Rightarrow dN &= \frac{Vk^2}{\pi^2} \frac{m}{\hbar^2 k} dE \\ &= \frac{mV}{\hbar^2 \pi^2} \sqrt{\frac{2mE}{\hbar^2}} dE \\ &= \frac{V}{2\pi^2} \left(\frac{2m}{\hbar^2}\right)^{3/2} \sqrt{E} dE & \Rightarrow g(E) &= \frac{V}{2\pi^2} \left(\frac{2m}{\hbar^2}\right)^{3/2} \sqrt{E} \end{aligned}$$

The  $E^{1/2}$  dependence (specific to 3D crystals) will become particularly important. At  $T = 0$ , electrons will be filled in states of as low an energy (and thus  $k$ ) as possible while abiding by PEP. Let the maximum occupied  $k$  at  $T = 0$  be called  $k_f$ , then we have:

$$N = 2 \frac{4\pi k_f^3/3}{8\pi^3/V} = \frac{Vk_f^3}{3\pi^2} \Rightarrow k_f = \left(\frac{3\pi^2 N}{V}\right)^{1/3} = (3\pi^2 n)^{1/3}$$

where  $n$  is the electron density. We define the Fermi energy  $E_F$  as the highest-energy state occupied at absolute zero. This is simply given by:

$$E_F = \frac{\hbar^2 k_f^2}{2m} = \frac{\hbar^2}{2m} (3\pi^2 n)^{2/3}$$



## 4.1 Heat Capacity

For  $T > 0$ , however, it is not simply the case that the electrons will simply be located in the lowest-energy states available to them. Rather, electrons are distributed according to the *Fermi-Dirac distribution*: the probability of a state of energy  $E$  being occupied at temperature  $T$  is:

$$p_f(E; T) = \frac{1}{1 + \exp\left(\frac{E-\mu}{kT}\right)}$$

where  $\mu$  is the *chemical potential*, which only has a small temperature dependence, and is the energy at which a state has a 50% chance of occupation. The number of states between  $E$  and  $E + dE$  which are actually occupied is therefore:

$$g(E)p_f(E; T) dE = \frac{V}{2\pi^2} \left(\frac{2m}{\hbar^2}\right)^{3/2} \frac{\sqrt{E}}{1 + \exp\left(\frac{E-\mu}{kT}\right)} dE$$

The multiplication of  $p_f(E; T)$  effectively “smears” out  $g(E)$  within about  $kT$  of  $\mu$ . We finally then obtain:

$$U_{\text{el}} = \int_0^\infty E g(E) p_f(E; T) dE = \frac{V}{2\pi^2} \left(\frac{2m}{\hbar^2}\right)^{3/2} \int_0^\infty \frac{E^{3/2}}{1 + \exp\left(\frac{E-\mu}{kT}\right)} dE$$

From which we can obtain:

$$C_{\text{el}} \equiv \frac{\partial U}{\partial T} \approx \frac{\pi^2}{2} N k \frac{T}{T_F}$$

where  $T_F$ , the *Fermi temperature*, is defined by  $k_B T_F = E_F$ . Usually  $T/T_F \approx 0.01$  for most metals at room temperature. Note that  $C_{\text{el}} \propto T$ . An alternative derivation considers the fact that the only electrons which are likely to be thermally excited are those within  $kT$  of  $\mu$ , of which there are about  $g(E_F)$ . Attributing a classical thermal energy of  $\frac{3}{2}kT$  to each, we obtain:

$$\begin{aligned} U' &= \frac{3}{2} \frac{V}{2\pi^2} \left(\frac{2m}{\hbar^2}\right)^{3/2} \sqrt{E_F} k^2 T^2 \\ \Rightarrow C_{\text{el}} &\approx \frac{3V}{2\pi^2} \left(\frac{2m}{\hbar^2}\right)^{3/2} \sqrt{E_F} k^2 T \end{aligned}$$

which is proportional to  $T$ , but it would be nice to have  $C \propto N$ . Note that:

$$N = \int_0^{E_F} g(E) dE = \frac{V}{2\pi^2} \left(\frac{2m}{\hbar^2}\right)^{3/2} \int_0^{E_F} \sqrt{E} dE$$

$$\begin{aligned}
&= \frac{2V}{6\pi^2} \left( \frac{2m}{\hbar^2} \right)^{3/2} E_F^{3/2} \\
\Rightarrow \frac{9N}{2E_F} &= \frac{3V}{2\pi^2} \left( \frac{2m}{\hbar^2} \right)^{3/2} \sqrt{E_F} \\
\Rightarrow C_{\text{el}} &\approx \frac{9N}{2E_F} k^2 T = \frac{9Nk}{2} \frac{T}{T_F}
\end{aligned}$$

which is quite close to the more rigorous value ( $\pi^2$  rather than 9).

The free electron model works surprisingly well, despite completely ignoring the crystal lattice. Discrepancies between this model and experiment are often accounted for by adjusting the electron mass to a “relative mass”  $m^*$ , which arises due to the lattice (see later).

Recall that the heat capacity due to the lattice vibrations was proportional to  $T^3$  at low  $T$ ; that due to the electrons has just been shown to be proportional to  $T$ . The overall heat capacity is then given by:

$$C = \frac{12\pi^4}{5} Nk \left( \frac{T}{\theta_D} \right)^3 + \frac{9}{2} Nk \frac{T}{T_F} = \beta T^3 + \gamma T$$

$\beta$  and  $\gamma$  (and thus the Debye and Fermi Temperatures) may be calculated experimentally by plotting  $C/T$  against  $T^2$ .

## 4.2 Bulk Modulus

Compressing a metal raises the energy of all the electron states, as they are forced to have a shorter wavelength to fit in the box. The electrons in the metal can thus be thought of as exerting an outward pressure, given by  $-\frac{\partial U}{\partial V}$ . This can be calculated very simply at  $T = 0$ . We recall that:

$$g(E) = \frac{V}{2\pi^2} \left( \frac{2m}{\hbar^2} \right)^{3/2} \sqrt{E} \propto E^{1/2} \quad E_F = \frac{\hbar^2}{2m} (3\pi^2 n)^{2/3} \propto V^{-2/3}$$

The average energy of a single electron at  $T = 0$  is given by:

$$\begin{aligned}
\langle U \rangle &= \frac{\int_0^{E_F} E g(E) dE}{\int_0^{E_F} g(E) dE} = \frac{\int_0^{E_F} E^{3/2} dE}{\int_0^{E_F} E^{1/2} dE} = \frac{\frac{2}{5} E_F^{5/2}}{\frac{2}{3} E_F^{3/2}} \\
&= \frac{3}{5} E_F
\end{aligned}$$

and so the pressure is given by:

$$p = -\frac{\partial N \langle U \rangle}{\partial V} = -\frac{3}{5} N \frac{\partial E_F}{\partial V} = -\frac{3}{5} N \left( -\frac{2}{3} \frac{E_F}{V} \right)$$

$$= \frac{2}{5}nE_F \propto V^{-5/3}$$

and the isothermal bulk modulus, defined by  $K_T \equiv -V\left(\frac{\partial p}{\partial V}\right)_T$ , by:

$$\begin{aligned} K_T &\equiv -V\frac{2}{5}N\left(\frac{\partial E_F/V}{\partial V}\right)_T = -V\frac{2}{5}N\left(-\frac{5}{3}\frac{E_F}{V^2}\right) \\ &= \frac{2}{3}nE_F \end{aligned}$$

### 4.3 Conductivity

The mean time between collisions (with either phonons or defects) is given by  $\tau$ , that is, the probability that by time  $t$  an electron hasn't collided with anything is  $e^{-t/\tau}$ . The rates due to phonons and defects individually can be added to give the total:  $\tau^{-1} = \tau_{\text{ph}}^{-1} + \tau_{\text{def}}^{-1}$ . If one assumes that the average velocity after a collision is 0, then one simply calculates the mean velocity as  $\langle v \rangle = ve^{-t/\tau}$ , which obeys:

$$\frac{d\langle v \rangle}{dt} = -\frac{\langle v \rangle}{\tau}$$

This is how the “drag” acceleration due to collisions is described in the FEM. The overall equation of motion for an electron (effective mass  $m^*$ ) in some fields is then:

$$m^*\dot{\mathbf{v}} = -e(\mathbf{E} + \mathbf{v} \times \mathbf{B}) - m^*\frac{\mathbf{v}}{\tau}$$

Suppose first that there is no  $\mathbf{B}$  field, and that the electrons are moving along in a steady current at a *drift velocity*, so that  $\mathbf{v} = \mathbf{v}_d$ ,  $\dot{\mathbf{v}} = \mathbf{B} = \mathbf{0}$ :

$$m^*\frac{\mathbf{v}_d}{\tau} = -e\mathbf{E} \Rightarrow \mathbf{v}_d = -\frac{e\tau}{m^*}\mathbf{E}$$

We also define *electron mobility*  $\mu \equiv v_d/E = e\tau/m^*$  here. Further, the current density is given by  $\mathbf{J} = -ne\mathbf{v}_d$ , and given that  $\mathbf{J} = \sigma\mathbf{E}$ , we obtain:

$$\mathbf{J} = \frac{ne^2\tau}{m^*}\mathbf{E} \Rightarrow \sigma = \frac{ne^2\tau}{m^*} = ne\mu$$

At low  $T$ , few phonons are excited in the metal, and so  $\tau$  is not infinite purely due to scattering with defects. The rate of defect scattering does not change with temperature (and so neither does  $\sigma$  at low  $T$ ), but different samples will have different numbers of defects and so will be offset from each other.

At high  $T$ , the number density of phonons becomes proportional to the temperature, and so  $\tau \propto T^{-1}$ . As such,  $\sigma \propto T^{-1}$  at high  $T$  as well, but the defects remain, and so different samples will retain the offset from each other mentioned above – this is known as Matthiessen's Rule.

## 4.4 Optical Reflectivity

Optical frequencies are much higher than the scattering rate, so this can be ignored. If there is no  $\mathbf{B}$  field, then simply  $m^*\ddot{\mathbf{x}} = -e\mathbf{E}$ . For a sinusoidal  $\mathbf{E}$  field and  $\mathbf{x}$ , we obtain  $m^*\omega^2 x_0 = eE_0$ . Now the polarisability has two definitions:

$$\begin{aligned} P &= -n e x_0 = \chi \epsilon_0 E_0 \\ -\frac{n e^2}{m^* \omega^2 \epsilon_0} &= \chi \\ \Rightarrow 1 + \chi &= \epsilon = 1 - \frac{n e^2}{m^* \omega^2 \epsilon_0} = 1 - \frac{\omega_P^2}{\omega^2} \end{aligned}$$

where  $\omega_P^2 = n e^2 / m^* \epsilon_0$ . We see that when  $\omega > \omega_P$ ,  $\epsilon > 0$  which means that the metal is transparent to the light. When  $\omega < \omega_P$ ,  $\epsilon$  becomes negative, meaning that the electromagnetic wave becomes evanescent within the metal, which appears opaque and reflective. For metals,  $\omega_P$  is usually in the UV range, so they are typically reflective.

## 4.5 Thermal Conductivity

The reasoning behind  $\kappa = \frac{1}{3} C \langle c \rangle l$  remains valid for electrons, and so this is used to estimate the thermal conductivity due to the electrons in a metal. Recall:

$$C_{\text{el}} = \frac{\pi^2}{2} n k_B \frac{T}{T_F}$$

Now  $k_B T_F = E_F$ , which is the energy of the electrons at the edge of the Fermi sphere; we can attribute a ‘‘Fermi velocity’’ to these such that  $E_F = \frac{1}{2} m^* v_F^2$ . We can also write that  $\langle c \rangle = v_F$  and  $l = v_F \tau$  to get everything into the variables with which we are now familiar. Then we have:

$$\begin{aligned} \kappa &= \frac{1}{3} \cdot \frac{\pi^2}{2} n k_B \frac{T}{\frac{1}{2k_B} m^* v_F^2} \cdot v_F \cdot v_F \tau \\ &= \frac{\pi^2 n k_B^2 T \tau}{3 m^*} \end{aligned}$$

On comparison with the thermal conductivity from *phonons*, this value (from the *electrons* is much larger, as with experiment. At high temperatures, we see that because  $\tau \propto T^{-1}$ , thermal conductivity of metals is roughly constant, whereas for insulators  $\kappa \propto T^{-1}$  in this regime.

If we take the ratios of the thermal and electrical conductivities, we obtain:

$$\frac{\kappa}{\sigma} = \frac{\pi^2 n k_B^2 T \tau}{3 m^*} \frac{m^*}{n e^2 \tau} = \frac{\pi^2 k_B^2 T}{3 e^2}$$

which is:

- Completely independent of the metal itself ( $m^*, n, \tau$ )
- Proportional to temperature, with constant  $L \approx 2.45 \times 10^{-8} \text{W } \Omega \text{K}^{-2}$

This was already an experimental law (the *Wiedemann-Franz Law*), and there is very good agreement.

## 4.6 Hall Effect

When a  $\mathbf{B}$  field is applied perpendicular to the current in a conductor, a potential difference (and thus  $\mathbf{E}$  field) is created in a direction perpendicular to both. In the steady state, we have:

$$\mathbf{E}_H = \mathbf{B} \times \mathbf{v}_d = -\frac{1}{ne} \mathbf{B} \times \mathbf{J} = R_H \mathbf{B} \times \mathbf{J}$$

where  $R_H$ , the *Hall coefficient*, is given by  $-1/ne$ . However, this is not in very good agreement with experiment, where  $R_H$  is sometimes positive, particularly for divalent metals (see later).

## 5 The Nearly-Free Electron Model

The Nearly-Free Electron Model differs from its totally free counterpart in that the lattice is not ignored – the electrons are treated as being in a potential with the lattice periodicity.

### 5.1 Bloch's Theorem

As with all other physical variables,  $|\Psi|^2$  must have lattice periodicity, and so we must have  $\Psi(\mathbf{r} + \mathbf{a}) = \Psi(\mathbf{r})e^{i\delta} = \Psi(\mathbf{r})e^{i\mathbf{k}\cdot\mathbf{a}}$  for an electron of wavevector  $\mathbf{k}$ . Therefore, the wavefunction in a crystal must be of the form:

$$\Psi_{\mathbf{k}}(\mathbf{r}) = u_{\mathbf{k}}(\mathbf{r})e^{i\mathbf{k}\cdot\mathbf{r}}$$

where  $u_{\mathbf{k}}(\mathbf{r})$  also has the lattice periodicity. This is *Bloch's Theorem*.

Retreating to 1 dimension and a box width of  $A$ , Bloch's Theorem gives:

$$\begin{aligned} u_k(x) &= \sum_{n=-\infty}^{\infty} C_{kn} \frac{1}{\sqrt{A}} e^{i\frac{2\pi n}{a}x} \\ &= \sum C_{kn} \frac{1}{\sqrt{A}} e^{inG_1x} \end{aligned}$$

$$\begin{aligned}
\Rightarrow \Psi(x) &= u_k(x) e^{ikx} \\
&= \sum C_{kn} \frac{1}{\sqrt{A}} e^{i(k+nG_1)x} \\
&= \sum C_{kn} |\phi_{kn}\rangle
\end{aligned}$$

where  $|\phi_{kn}\rangle = \frac{1}{\sqrt{A}} e^{i(k+nG_1)x}$  are the set of basis states that will be used. The state  $|\phi_{k0}\rangle$  is a free electron with wavenumber  $k$ .

Similar considerations mean that the potential  $V(x)$  is given by:

$$V(x) = \sum_{p=1}^{\infty} V_p \cos(pG_1x) = \sum_p \frac{V_p}{2} (e^{ipG_1x} + e^{-ipG_1x})$$

where the origin is the location of an ion, and we have taken  $V_0 = 0$ .

## 5.2 Matrix Mechanics

The Schrödinger Equation gives:

$$\begin{aligned}
\sum_m C_{km} \hat{H} |\phi_{km}\rangle &= E \sum_p C_{kp} |\phi_{kp}\rangle \\
\sum_m \underbrace{\langle \phi_{kn} | \hat{H} | \phi_{km} \rangle}_{H_{nm}} C_{km} &= EC_{kn}
\end{aligned}$$

which is a matrix equation. We should first calculate the matrix elements  $H_{nm}$ :

$$\begin{aligned}
H_{nm} &= \int_0^A \frac{1}{\sqrt{A}} e^{-i(k+nG_1)x} \left( -\frac{\hbar^2}{2m_e} \frac{\partial^2}{\partial x^2} + \sum_p \frac{V_p}{2} (e^{ipG_1x} + e^{-ipG_1x}) \right) \frac{1}{\sqrt{A}} e^{i(k+mG_1)x} dx \\
&= \frac{1}{A} \int_0^A \frac{\hbar^2(k+mG_1)^2}{2m_e} e^{i(m-n)G_1x} dx + \frac{1}{A} \sum_p \frac{V_p}{2} \int_0^A (e^{i(m-n+p)G_1x} + e^{i(m-n-p)G_1x}) dx \\
&= \frac{\hbar^2(k+mG_1)^2}{2m_e} \delta(m-n) + \sum_p \frac{V_p}{2} [\delta(m-n+p) + \delta(m-n-p)]
\end{aligned}$$

The nearly-free electron model posits that the only significantly contributing to a state with wavenumber  $k$  will be  $|\phi_{k0}\rangle$  and  $|\phi_{k-1}\rangle$  (or perhaps  $|\phi_{k1}\rangle$ ), that is:

$$|\Psi\rangle \approx C_{k0} |\phi_{k0}\rangle + C_{k-1} |\phi_{k-1}\rangle$$

This is justified by saying that for a small potential, only states with energies close to that of the central basis state  $|\phi_{k0}\rangle$  (whose energy is  $\hbar^2 k^2 / 2m$ ) will

have significant contributions to the overall wavefunction. As  $E \propto (k+nG_1)^2$ , any states other than these two will be much higher in energy.

For small values of  $k$ , even the adjacent  $|\phi_{k-1}\rangle$  state will be significantly higher in energy, and  $C_{k-1} \approx 0, |\Psi\rangle \approx |\phi_{k0}\rangle$ . For a value of  $k$  near the 1BZ boundary, the two will have a more comparable energy; the energies are equal for  $k = G_1/2$  and here the two states contribute equally.

With only these two states, the only matrix elements that are required are  $H_{00}, H_{0-1}, H_{-10}, H_{-1-1}$ :

$$\begin{aligned} H_{-1-1} &= \frac{\hbar^2(k - G_1)^2}{2m_e} \equiv E_{k-1} & H_{0-1} &= \frac{V_1}{2} \\ H_{00} &= \frac{\hbar^2 k^2}{2m_e} \equiv E_{k0} & H_{-10} &= \frac{V_1}{2} \end{aligned}$$

so we have:

$$\begin{pmatrix} E_{k-1} & V_1/2 \\ V_1/2 & E_{k0} \end{pmatrix} \begin{pmatrix} C_{k-1} \\ C_{k0} \end{pmatrix} = E_k \begin{pmatrix} C_{k-1} \\ C_{k0} \end{pmatrix}$$

an eigenvalue equation with the solution:

$$\begin{aligned} E_k &= \frac{1}{2}(E_{k-1} + E_{k0}) \pm \sqrt{\frac{1}{4}(E_{k-1} - E_{k0})^2 + \left(\frac{V_1}{2}\right)^2} \\ &= \frac{\hbar^2}{4m_e}((k - G_1)^2 + k^2) \pm \sqrt{\left(\frac{\hbar^2}{4m_e}((k - G_1)^2 - k^2)\right)^2 + \left(\frac{V_1}{2}\right)^2} \end{aligned}$$

### 5.3 Bands and Conduction

$E_{k-1}$  and  $E_{k0}$  are quadratic functions of  $k$ , offset from one another by  $G_1$ ; when  $V_1 = 0$ , the two branches of  $E_k$  are simply these two quadratics. However, when  $V_1 \neq 0$ , the two branches separate, forming two distinct *bands*.

More generally, when one considers more basis states  $|\phi_{kn}\rangle$  and more Fourier components of  $V(x)$ , more bands are formed, with gaps between them. The Fermi energy determines which bands are occupied – and to what extent.

When there is no electric field, electrons are all simply in the lowest state possible, and due to the symmetry of the bands there are equal numbers moving forwards ( $\frac{\partial\omega}{\partial k} > 0$ ) as backwards, so there is no net current. When an electric field is applied, however, electrons are forced into higher  $k$ -states in one direction, leading to a net current. Interactions with phonons and defects will cause some electrons to be scattered into states with similar  $|\mathbf{k}|$ ,

but with a randomised direction, so after thermalising down in energy they often end up at the back of the queue.

In one dimension, the separation between electron states in  $k$ -space is  $2\pi/X$  and the Brillouin zone has a size  $2\pi/a$ ; there are therefore  $X/a = n$  electron states, and each band therefore has a capacity of  $2n$ . For a univalent element, the first band is half-filled, which means that the electrons can be displaced over to one side of the band (in  $k$ -space) by an electric field – univalent elements are conductors. For a trivalent element, the first band is totally full, and the second band is half-filled – trivalent elements also conduct.

It might be expected that divalent elements would not conduct, as they would have a full first band and an empty second band, neither of which can have their electrons displaced by an electric field. However, this is only the case in 1D. It is always the case that for divalent metals, there are *enough* electrons to fill the first band and leave no other states occupied, but it can be seen that in 2D, the highest states in the first band (those with  $\mathbf{k}$  near the corner of the 1BZ) can in fact be *higher* in energy than the lowest states in the *second* band, if the potential is not too strong as to cause a large separation between the two bands. As a result, the first band is sometimes only *almost* full, and the second only *almost* empty.

### 5.3.1 Bloch Oscillations

If the field is strong and the scattering weak, the filled states may be able to cross into the 2BZ – i.e. backfolded into the back of the 1BZ. The effect of this is an oscillating current, known as *Bloch oscillation*. The time period of these oscillations can be derived by noting that the forcing of an electric field  $E$  is  $-eE$ , which will be equal to  $\hbar \frac{dk}{dt}$ , where the derivative is the rate at which the  $k$  of any particular electron is changing. The time period is then the size of the 1BZ divided by  $\frac{dk}{dt}$ .

Bloch Oscillations are observable in both condensed matter and in ultra-cold Cs atoms.

### 5.3.2 Effective Mass

Sometimes forces can have unexpected effects on electrons in bands, which is accounted for by ascribing to the electrons an *effective mass*  $m^*$ . We have:

$$m^* \dot{v} = \dot{p}$$

$$m^* \frac{d}{dt} \left( \frac{1}{\hbar} \frac{dE}{dk} \right) = \hbar \frac{dk}{dt}$$



$$m^* \frac{dk}{dt} \frac{d^2 E}{dk^2} = \hbar^2 \frac{dk}{dt}$$

$$\Rightarrow m^* = \hbar^2 / \frac{d^2 E}{dk^2}$$

In higher-D crystals it is clear that electrons may have different effective masses in different directions: at saddle points of the dispersion relation the electrons have positive mass in one direction and negative mass in the other!

Effective masses can be directly measured by applying strong magnetic fields to a metal, which causes electrons to resonate around the field lines with frequency

$$\omega = \frac{eB}{m^*}$$

This must be very high, as otherwise the electrons will collide with phonons or impurities before travelling most of a circle. Strong  $B$  fields and low temperatures are required to enable the electrons to travel for as long as possible, and the resulting frequencies are often in the high-frequency radio range (GHz). This technique is *cyclotron resonance*.

### 5.3.3 Holes

Divalent metals have an almost full lower band (known as the *valence band*) and an almost empty upper band (the *conduction band*). Rather than accounting for the movement of all the electrons in the valence band, it can be easier to think of this as being equivalent to a *full* valence band superimposed with a small number of *holes*. These holes have the negative of the energy of the electrons (the *hole band* is inverted with respect to the valence band) and the negative of the momentum as well.

One reason that using holes is convenient is that at the top of the valence band the curvature is negative, leading to a negative effective mass. Holes do not suffer from this: the hole corresponding to the lack of an electron with a negative effective mass has a positive mass, making it far easier to think about.

Both electrons and holes contribute to electrical conductivity, so we have for instance:

$$\sigma_{\text{tot}} = \sigma_e + \sigma_h = \frac{n_e e^2 \tau_e}{m_e^*} + \frac{n_h e^2 \tau_h}{m_h^*}$$

The effective mass of the holes  $m_h^*$  can also be measured by cyclotron resonance (above).

Also, a more accurate value for the Hall coefficient can be deduced, involving both electron and hole properties, which accounts for some of the discrepancies seen earlier.

## 6 Semiconductors

Unlike in divalent metals, the top of the valence band of a semiconductor is below the conduction band, so at  $T = 0$  there is no conduction. However, this gap is small enough that at  $T > 0$  some charge carriers can jump the gap thermally; silicon is a classic example of such a material. When made of a pure substance, the semiconductor is described as *intrinsic*, but it can also be *doped* with impurities such as phosphorus or aluminium, forming an *extrinsic* semiconductor, which will be the subject of this section.

### 6.1 Doping

When one replaces some Si atoms with P atoms, the energy levels change only slightly, so the band structure looks the same. P is however in group 5, so there is an extra electron that has been donated to the system. This electron can either be in an *ionised state* – away from the P atom and in the conduction band – or a *bound state* AKA *donor state* – orbiting the  $P^+$  in a quasi-hydrogenic orbit, for which:

$$E = -\frac{m^* e^4}{32\pi^2 \epsilon^2 \epsilon_0^2 \hbar^2} \qquad r = \frac{4\pi \epsilon \epsilon_0 \hbar^2}{m^* e^2}$$

This energy is relative to the electron being free to move in the conduction band. It is clearly independent of  $k$ , and so these bound states are often drawn as straight lines underneath the conduction band; they are often only about  $-0.01\text{eV}$  so they're certainly closer to the conduction band than the valence band.

P brings an extra electron to proceedings, so it is described as an *n-type dopant*. Al, by contrast, is in group 3, so if Si is replaced by Al there is a *hole* introduced; Al is a *p-type dopant*. As with the electron donated by P, this hole can either be in an ionised state or a bound state AKA *acceptor state*, being either far away or orbiting an  $Al^-$  ion. Analogously, the bound state is located slightly above the valence band. [In fact what has *actually* happened is that in the “ionised” state the Al has stolen an electron from the valence band, leaving a free hole in the valence band; in the bound state the Al re-releases this electron (a higher-energy state) and the hole becomes “bound”]

### 6.2 Chemical Potential

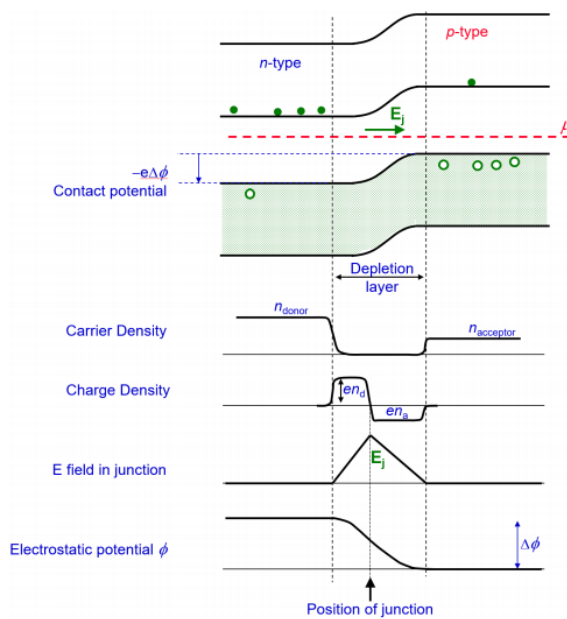
From the Fermi-Dirac distribution above, it can be seen that  $\mu$  is the energy at which a state has a 50% chance of being occupied by an electron. At

$T = 0$  therefore, when all the lowest-energy states are occupied, a p-type semiconductor has  $\mu$  at a level in between the occupied donor states and the unoccupied valence band, and an n-type semiconductor has  $\mu$  in between the full valence band and the unoccupied (i.e. full of holes) acceptor state.

As  $T$  increases, however, higher energy states will become occupied due to thermal excitation. P-type semiconductors will have their donor electrons excited to the conduction band (becoming unbound) [note:  $kT \approx 0.025\text{eV}$  at  $T = 300\text{K}$ ], as will some valence electrons; the chemical potential decreases as the donor state is likely unoccupied. N-types will have their valence electrons excited into the acceptor state, as well as perhaps the conduction band. The chemical potential increases as the acceptor state becomes occupied as well as the conduction band a bit. In both cases,  $\mu$  moves towards the gap between valence and conduction bands; as  $T \rightarrow \infty$  the  $\mu$  will equalise as in this regime electrons don't care about what states are available.

### 6.3 PN Junctions

Even at finite temperature, the chemical potential of an n-type semiconductor is higher than that of a p-type. If the two are brought into intimate contact, electrons will therefore diffuse from n to p, leaving  $\text{P}^+$  ions behind in favour of the lower-energy unoccupied p-type valence states. Eventually however, the charge imbalance sets up a *contact potential* difference which balances the initial chemical potential difference.



The result is shown left. Electrons from n diffuse over to p, depleting some of its holes. This creates a *depletion layer* across the junction, containing no charge carriers but net charges on either side of the junction. As  $\nabla \cdot \mathbf{E} = \rho/\epsilon\epsilon_0$ , this creates an electric field within the depletion region, directed from n to p (as n has now lost a lot of negative charges and become positive). Further, as  $\mathbf{E} = \nabla\phi$ , there is an electrostatic potential created, which mirrors the chemical potential difference, so they cancel out overall and equilibrium is

reached.

### 6.3.1 Biases and Diodes

If one manually applies a potential difference across the PN junction, the effect is different depending on the direction of the potential difference.

If the junction is *forward biased*, we are pushing the electrons in the direction they wanted to flow before the junction was created – from n to p. This means that the electrons in the conduction band of the n-type material are forced towards the junction to combine with more holes (as are the holes in the valence band of the p-type) creating a “recombination current”; there are a lot of these carriers and so conduction is good in this direction. This bias causes the depletion region to increase as more electrons are being enlisted to travel across the junction.

In *reverse bias*, the voltage is applied the other way. The charge carriers mentioned above (the “majority carriers”) are forced away from the boundary, and the much smaller number of electrons in the conduction band of the n-type (and holes in the valence band of the n-type) are forced across. The current generated as a result (“generation current”) is far smaller.

These currents can be quantified. Consider  $E \gg \mu$ ; the Fermi-Dirac distribution then gives:

$$p(E) = p_f(E; T) = \frac{1}{1 + \exp\left(\frac{E-\mu}{kT}\right)} \approx \exp\left(\frac{\mu - E}{kT}\right)$$

When  $\mu$  is artificially increased to  $\mu + eV$ , we obtain:

$$p(E; V) = p(E; 0) \exp\left(\frac{eV}{kT}\right)$$

At  $V = 0$ , the generation current is equal to the recombination current (hence steady state) and the generation current doesn’t vary with voltage or temperature. On the other hand, the recombination current *does*, it is proportional to  $\exp(eV/kT)$ . As such, the total current is:

$$I = I_0 \left[ \exp\left(\frac{eV}{kT}\right) - 1 \right]$$

This gives essentially a one-way current – this is a *diode*.

## 6.4 Semiconductor Devices

Using the ideas developed above, many common semiconductor devices can be qualitatively understood, including the Zener diode, avalanche breakdown diodes, LEDs, semiconductor lasers, and solar cells.

### 6.4.1 Zener Diodes

If the reverse bias is strong enough, the energy at the top of the p-type valence band is higher than the bottom of the n-type conduction band. This enables electrons in the p to quantum tunnel through to the other side.

This requires the materials to be heavily doped, so that the chemical potential is very close to the band edge. The Zener breakdown depends on the amount of doping, but often requires more than 3V. Whatever the breakdown voltage is, it is usually very reliable, and so Zener diodes are often used as references.

### 6.4.2 Avalanche Breakdown

Strong reverse bias might also cause a different kind of breakdown – avalanche. Thermal excitation may cause some carriers within the depletion region to un-deplete and get moving again. As they do so, collisions will often cause other un-depletions, generating  $e^-$ - $h^+$  pairs; eventually a large reverse current flows. This process dissipates lots of heat and can damage the device. The avalanche may be triggered by a single photon, and so diodes in reverse bias can be used as single-photon detectors.

### 6.4.3 LEDs

When a PN junction is forward-biased, majority carriers flow into the depletion region and combines with holes; this process releases energy. For “direct band-gap” materials (ideal for LEDs), this is most likely to be in the form of light; the size of the band gap determines the wavelength of light emitted. For *indirect* band-gap materials, light emission requires momentum from a phonon, making it more likely that the energy will simply be dissipated as heat.

LEDs are useful for communications, as they can be turned on and off very quickly; they are also more energy-efficient than incandescent or fluorescent lights.

### 6.4.4 Lasers

Ordinarily, higher energy states are less likely to be occupied (Boltzmann), but if a *population inversion* can be maintained, they can be forced to be *more* likely to be occupied. This is done by electrical “pumping”, using a strong forward bias; this relies on the chemical potential being within the n-conduction and p-valence bands, which requires very heavy doping. The junction is then placed in an optical cavity, wherein photons of the band-gap

energy bounce back and forth. These photons are able to stimulate electronic transitions between the upper states and the lower states, leading to more photons being produced.

#### **6.4.5 Solar Cells**

Solar cells are basically reverse LEDs. Solar photons create carrier pairs in the depletion region, which are swept away by an electric field. Again, heavy doping is required.